Belov I., Le Goff S., Nesterov A., Quenez J.M., Shaposhnikov V.

Calculation of the vibro-displacements governing fatigue strength of membrane containment systems under operation in Arctic ice for Arc6 180,000 m^3 LNG carrier

ABSTRACT

The study has been performed to describe the vibration of the membrane containment system of a liquefied natural gas carrier (LNGC) under operation in Arctic conditions. Conservative assumptions have been taken in order to identify an upper bound of vibro-displacements for a membrane-type LNGC with Ice class notation Arc6. A 180,000 m^3 LNGC is considered with slow speed propulsion, icebreaking bow and twin propellers.

The paper will describe the hypotheses, the method to estimate the ice loads, the calculations and the results in terms of vibration. The ice excitation on the hull is considered together with propeller and engine induced vibration in order to cover all the possible excitations that occur during ice navigation.

The results obtained with a parametric generic ship of highest Ice class notation are mandatory in order to assess the capacity of the containment system to withstand vibrations due to LNGC Arctic operations, prior to specific approval for a specific project.

1. STATEMENT OF THE PROBLEM

In connection with the necessity to transport natural gas from the Arctic shelf and coast of Russia, the problem of developing large Arctic LNGC, able to operate in the Barents Sea, but also in the more severe conditions of the Kara Sea, and, in prospect, on the whole Northern Sea Route (NSR), has become necessary. The present work seeks to demonstrate that membrane LNGC are suitable for such transportation. To demonstrate correctness of GTT technologies for providing sufficient life under vibration due to ice - hull interaction effects, as well as additional induced vibration caused by screw propeller - ice interaction and main engine operation in ice conditions, a work package on theoretical and experimental study of these issues was performed.

At first, the concept-project of an Arc6 class notation LNGC with capacity 180,000 m^3 was developed. Subsequently, the exciting forces under ice operation were analyzed and the ship vibration was calculated by finite element analysis. The vibration analysis was performed for

the ship operation under full loading (all tanks fully filled) and under minimum loading (all tanks empty except tank n°4 filled at 10% of height). This permitted the definition of the vibration displacement spectra and the development of the test program.

Secondly, static and endurance tests of a full scale mock-up representative of NO96 membrane cargo containment system (CCS) were conducted. The tests were aimed to evaluate the actual fatigue strength margins of NO96 membrane containment system and perform spectral analysis of vibration in the frequency range corresponding to service conditions of Arc6 LNGC.

2. DEFINITION OF HULL SHAPE AND MAIN STRUCTURAL ELEMENTS

The level of vibro-displacements depends on ice operation conditions, as well as the shape and structure of the LNGC hull. Taking into consideration that at the present time there is no project of LNGC of highest class notations, the main elements of LNGC hull of high ice class notation Arc6 with four cargo tanks having the total capacity about 180,000 m^3, with slow-speed diesel-engines, icebreaker bow and two variable-pitch screw propellers were designed as the first step. The general view and main dimensions of this LNGC are shown in Fig.1.

The bow lines meet the requirements of Russian Maritime Register of Shipping (RMRS) Rules [1] to ships of Arc6 ice class notation. An ice tooth is provided in the stern area to protect the screw propellers against ice effects in case of backward operation. The developed hull shape provides minimum loads under the ship ice operation. The main structural elements are also designed according to the requirements of RMRS Rules and GTT design criteria for NO96 [2] and MKIII.

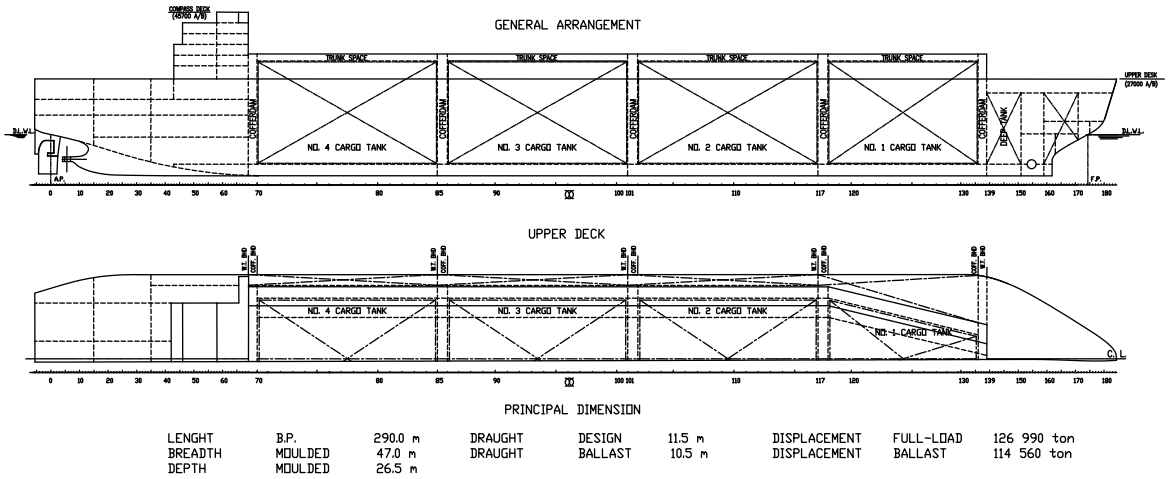

Fig. 1: The general view and main dimensions of Arc6 ice class notation LNGC with four cargo tanks having the total capacity 180,000 m^3, with slow-speed diesel-engines, icebreaker bow and two screw propellers

The bow area (A & A1 in Fig.2) of ice strengthening structures has a transverse framing system with web frames, load-carrying and load-separating stringers. This area is located over the whole side depth. The plating thickness is 30 mm.

The intermediate area (B in Fig.2) in general has a transverse framing system with web frames, load-carrying and load-separating stringers. A transverse framing system without web frames and stringers is applied in the bilge region (III in Fig.2). Two platforms and vertical diaphragms reinforced by stiffeners over the whole height are installed in this region. The mean plating thickness in this area is 28 mm.

The aft area (C in Fig.2) has a longitudinal framing system with additional frames at ½ of web frame spacing on the side and a transverse framing system on the bilge and bottom (III & IV in Fig.2). The mean plating thickness in this area is about 30 mm. Classification of ice strengthening areas is assumed as per RMRS Rules (Fig.2).

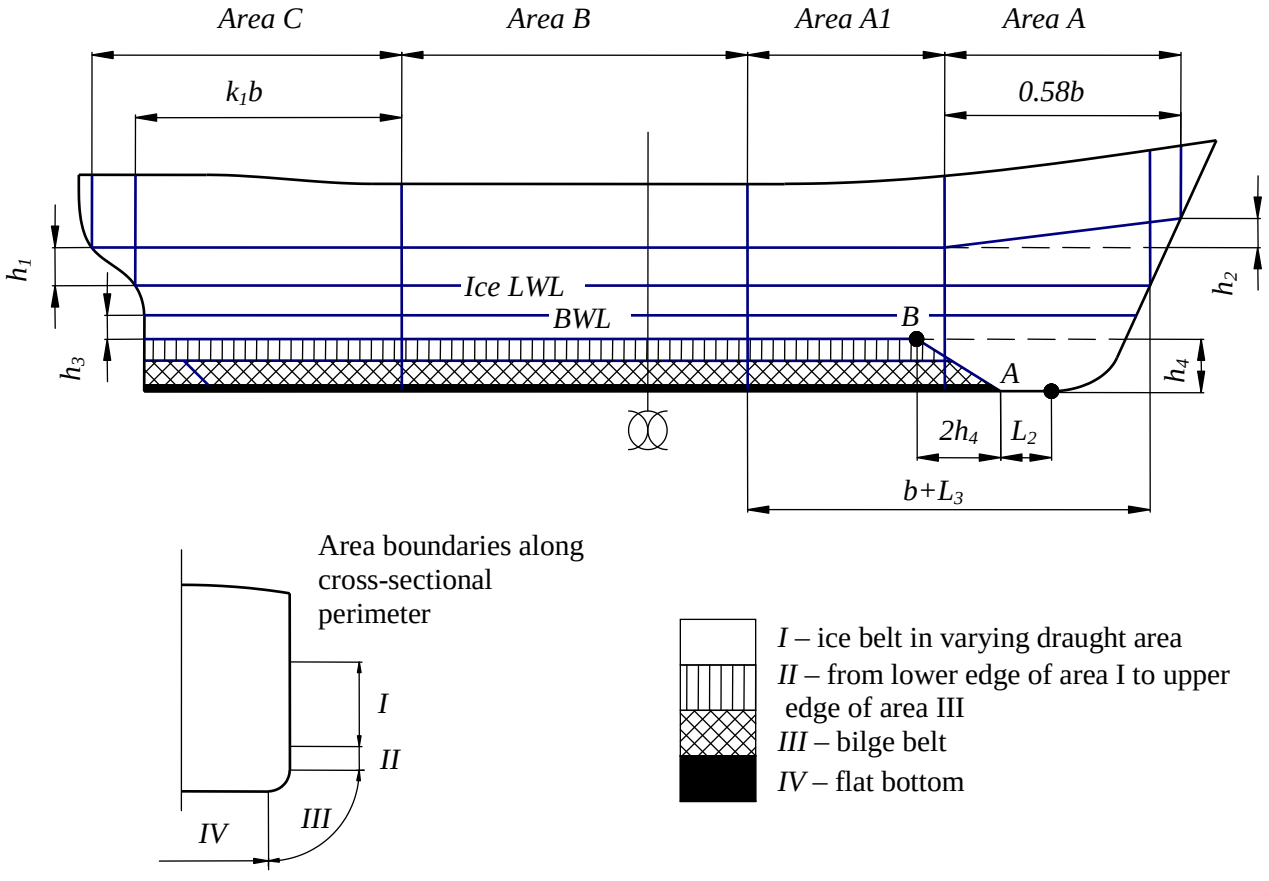

Fig. 2: Boundaries of ice strengthening areas

3. SELECTION OF DESIGN SHIP ICE OPERATION SCENARIOS AND EVALUATION OF ICE LOADS

When operating a vessel independently in the compact ice, sequential chipping of ice floes off the compact ice field takes place. Because the ship continues her forward operation and regains contact with the unbroken ice and breaks it, a cyclic load occurs. Therefore, the ice load potentially incorporates cyclic stresses that could induce fatigue damage. Another possible source of fatigue loads consists in post-impact vibration occurring after strong impacts against the ice. Being non-hazardous for the ship steel hull, these loads might cause damage in membrane systems of LNGC.

Non-standard situations occur during large LNGC operation in a canal after an icebreaker. Presently all existing icebreakers make canals, the width of which is lesser than the beam of potential large LNGC. Therefore, the canal width will be increased due to canal edge interaction with the large LNGC hull. This interaction in the form of periodic impacts resulting in bending failure of canal edge portions also produces cyclic loads to be withstood by membrane containment systems.

To evaluate fatigue ice loads occurring under ice operation, the following ice thicknesses, under which the ship could operate independently moving continuously, shall be defined: the maximum one h_{m1} and the one permitted by RMRS Rules h_{m2}, as well as ice thickness h_{m3} permitted by RMRS Rules for operation under icebreaker escort.

Based on the obtained values of h_{m1}, h_{m2}, h_{m3}, the maximum service ice thickness where ship operates independently (h_{n1}) and the maximum service ice thickness where ship is escorted by one icebreaker with finish ice canal breaking (h_{n2}) shall be specified.

When defining h_{n1} and h_{n2}, economical aspects and ice passability as well as restrictions imposed by RMRS shall be considered by meeting the following conditions:

$$h_{n1} \le h_{m1} \qquad h_{n1} \le h_{m2} \qquad h_{n2} \le h_{m3}$$

It shall be noted that assuming h_{n1} *equal to* h_{m1} could be disadvantageous by economic considerations as when the ice thickness is close to the ultimate ice passability, the ice operation speed normally does not exceed 2 ~ 3 knots.

After regulating values h_{n1} and h_{n2}, it could be assumed that ship independent operation takes place for ice thickness range [*0;* h_{n1}] and under one icebreaker's escort takes place for ice thickness range [h_{n1}*;* h_{n2}].

To regulate fatigue loads, each of the ranges shall be divided into stationary modes. By taking into consideration the ice load changeability level, it is recommended to divide the first range into three stationary modes. Provided the following condition is valid:

$$h_{n2} - h_{n1} \le \frac{h_{n1}}{2},$$

it is recommended to consider the second range as one stationary mode (the fourth one).

To evaluate the ship speed under independent ice operation stationary modes, a linear approximation of the ice passability curve could be used:

$$v(h_i) = v_{ow} - (v_{ow} - v_{\min})\frac{h_i}{h_{m1}}$$

where v_{min} - speed of ship independent operation in compact ice

v_{ow} - speed in open water

The reachable speed for the canal finish breaking shall be evaluated from tests in the ice model tank, but for the first approximation it could be taken as:

v_4 = 5 knots = 2.57 m/s.

A fifth mode concerns a wrong manoeuvre in thick ice. Regarding impacts against the thick ice that are hazardous in terms of post-impact vibration, an analysis has shown that the amplitude of such a load could be estimated from the formulae for the ultimate strength of the ice strengthening structures, and its effecting time as follows:

$$t = \frac{M.V_{red}}{P_{\max}} \cdot f_t(k)$$

where M - ship mass

V_{red} - ship speed reduced to the impact direction (projection of ship speed on the perpendicular to the impacted surface)

$P_{\max}$ - maximum interaction force if ice flexural failure is not provided

$f_t(k)$ - coefficient considering ice flexural failure

The final loading time history for mode 5 is a triangular transient force applied to one of the bow stations of the LNGC:

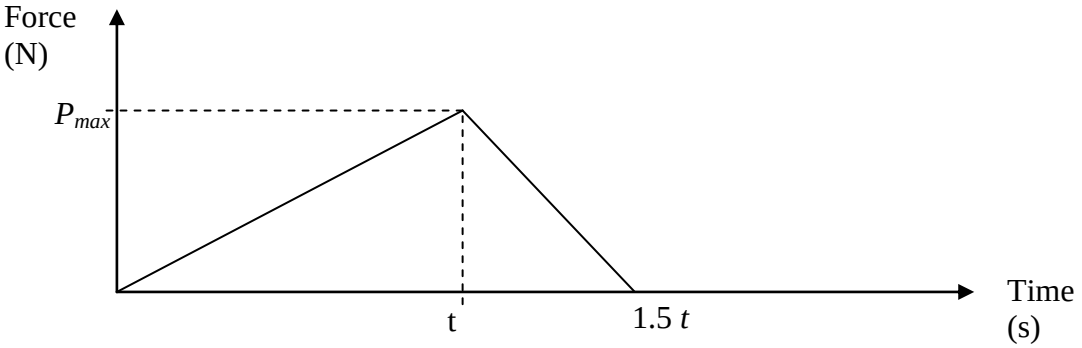

Fig. 3: Exciting force time history for mode 5

Based on the explained approach, the design modes given in Table 1 were taken for an LNGC of Arc6 ice class notation.

Table 1.

Parameters of design ice operation modes for ship under consideration

Mode No.	Ice operation type	Design ice thickness h_i (m)	Design operational speed v_i	
			knots	m/s
1	Independent	0.17	15.5	8.0
2	Independent	0.50	10.5	5.4
3	Independent	0.83	5.5	2.8
4	After one icebreaker	1.25	5.0	2.6
5	Impact against thick ice	4.00	6.6	3.4

To define ice load parameters for modes 1 to 4, the methodology [3] is used, which considers the ice edge angular shape and buoyancy forces of earlier submerged ice fragments moving together with the ship hull.

To define ice load parameters for mode 5, P_{max} and $f_t(k)$, special software is used, which realizes the algorithm of the hydrodynamic model of ship impacts against the ice [4] by base dangerous service conditions.

4. EVALUATION OF EXCITING FORCES DUE TO PROPELLERS AND ENGINES

The following three groups of exciting forces due to propellers and engines were considered: forces caused by screw propeller blades interaction with the ice and by screw propeller blades interaction with the water containing ice fragments, as well as forces caused by main engine operation.

The screw propeller having the following parameters was considered in the calculations:

Diameter D (m)	7.1
Number of blades	5
RPM under ice operation n (1/ min): for mode 1	105
for modes 2 to 5	90

To define the first group of the exciting forces, an approximate method based on statistical processing of model test results for ice-going ships [5, 6], as well as recommendations of RMRS were used.

The exciting forces on the blade caused by ice milling could be estimated as follows:

$$F^I = \begin{pmatrix} F_x^I = S \cdot (22 + 24e^{-0.17\alpha(r=0.9)}) \cdot D^{1.6} c_{mean} \sigma_{(r=0.8)} \\ F_y^I = 0.1 F_x^I \\ F_z^I = 0.1 F_x^I \end{pmatrix}$$

where S - factor dependent on operation mode

c_{mean} - mean dimensionless blade width for ice penetration portion

$\alpha(r = 0.9)$ - design angle of the blade attack on relative radius r=0.9 (deg)

$\sigma_{(r=0.8)}$ =3.2 MPa - compression ultimate ice strength

For vibration calculations, it is accepted that one screw (starboard, for example) interacts with an ice floe; the angle between the ice floe plane and centerline (CL) is equal to 0^0 which corresponds to the maximum vertical force or 90^0 which corresponds to the maximum transverse force. The variant of simultaneous interaction of both screws with the ice is improbable and is not considered.

The second group of exciting forces consists in F^h, the hydrodynamic exciting forces conditioned by screw operation in water mixed with ice which are determined by the methods recommended by RMRS [7].

The value of the total exciting forces $F_\sum$ due to propellers made up of hydrodynamic F^h and ice F^I components is defined by the following formula: $F_\sum = \sqrt{\left(F^I\right)^2 + \left(F^h\right)^2}$

The third group of forces includes the values of periodic moments of 2nd, 4th and 7th orders given in the design documentation for diesel engines considered as exciting forces caused by main diesel engine operation.

5. SOFTWARE AND DESIGN MODEL FOR GLOBAL VIBRATION ANALYSIS

General description

Finite element software ANSYS was employed for global hull vibration analysis. The 3-D design model (Fig. 4) generated on the base of ship design documentation was used. The masses of structures, ballast and machinery are considered in the density of the finite element material, as well as with lumped masses.

Hull vibration damping coefficients strongly vary between open water and ice navigation. A direct experiment [10] with nuclear-powered icebreaker's hull vibration excited by shaker in the open water and in the ice of different thickness has demonstrated that an ice field surrounding the ship strongly increases the oscillation power dispersion. The damping coefficient is defined by the following formula:

$$\zeta = 0.001\ \pi\lambda_6$$

where λ_6 is natural frequency of 6th mode of hull vertical vibration.

The points where vibration displacements caused by ice bow-ice interaction were defined are shown in Fig. 5.

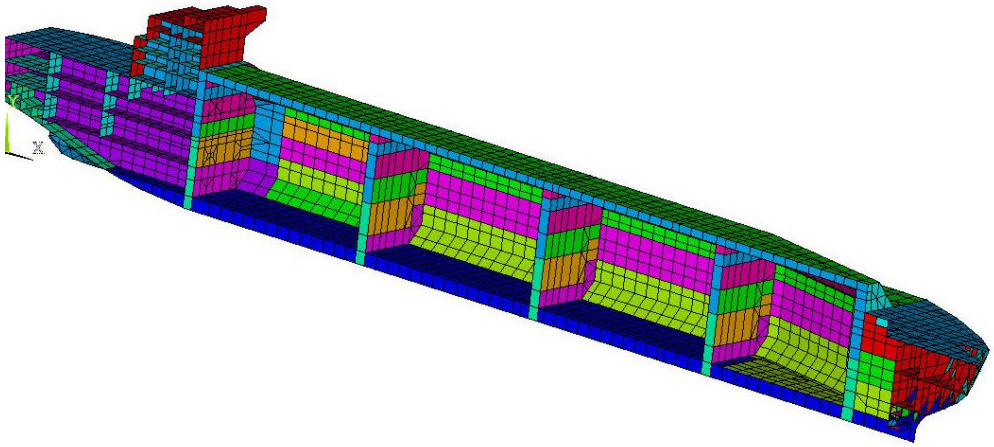

Fig. 4: Finite element model

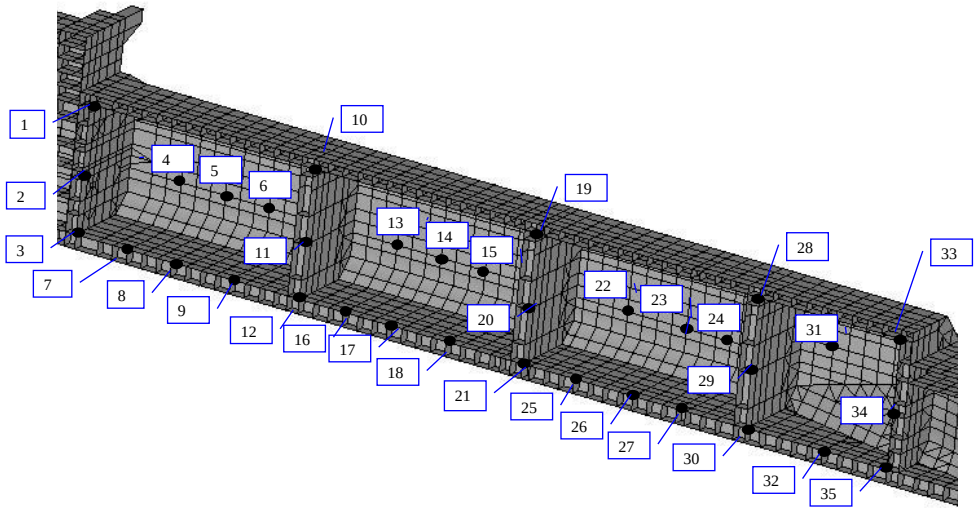

Fig. 5: Design points for calculating vibration displacements

The water added masses are considered by additional nodal masses. The added masses were calculated based on the analytic solution [8] ignoring ice effects. This assumption is corroborated by results of vibration full-scale experiments for middle size Arctic ships [9] which demonstrated that hull natural frequencies values affected by ice conditions vary within 1 to 5%; therefore, this phenomenon may be neglected for practical purposes.

Global vibration calculation for the ice-hull interaction excitation

The analysis for exciting forces caused by bow – ice interaction is made in the time domain with the help of ANSYS TRANSIENT analysis provided in software ANSYS. In this case, hull added masses correspond to hull first modes of vertical and horizontal vibrations (first bending mode in vertical plane is considered to determine added masses in the vertical direction on the nodes of the outer wetted surface, and first bending mode in horizontal plane is considered to determine added masses in the transverse direction on the same nodes).

Global vibration calculation for the propellers and engines excitations

The calculation of global vibration under forces induced by the propellers and main engines (exciting forces presented in §4) was performed for added masses of 5^{th} mode. The calculations for exciting forces caused by propeller and engine operation are performed in the frequency domain.

Liquefied gas added masses

In both cases (hull-ice interaction and propellers/engines excitations), the liquefied gas added masses were considered:

- in the longitudinal direction applied to transverse tank bulkheads wetted by the cargo on their both surfaces (added mass corresponding to first mode of bulkhead but equally distributed among the nodes),
- in the vertical direction, as the mass of the vertical column of liquid on the corresponding nodes located at the bottom of the tank (both inner and outer hulls as required by KSRI methodology),
- in the transverse direction, as the mass of the transverse column of liquid on the corresponding nodes located on the walls (both inner and outer hulls as required by KSRI methodology).

Selection of frequencies

The following independent responses were considered:

- responses due to propellers excitation in frequency domain (7.5 Hz for mode 1 and 8.75 Hz for modes 2 to 5; cf. Table 1)
- responses due to engines excitation in frequency domain (3.5, 7.0 and 12.25 Hz for 2^{nd}, 4^{th} and 7^{th} harmonics for mode 1 and 3, 6 and 10.5 Hz for 2^{nd}, 4^{th} and 7^{th} harmonics for modes 2 to 5; cf. Table 1)
- responses due to hull-ice interaction in the time domain decomposed on the following elementary frequencies (0.7, 1.3 Hz and all frequencies already considered previously)

Table 2.

Elementary frequencies and corresponding excitations considered

Frequencies (Hz)	Propellers	Engines	Hull
0.7			Decomposition of a time domain vibration calculation
1.3			
3		2nd harmonic of Mode 1	
3.5		2nd harmonic of Modes 2 to 5	
6		4th harmonic of Mode 1	
7		4th harmonic of Modes 2 to 5	
7.5	Mode 1		
8.75	Modes 2 to 5		
10.5		7th harmonic of Mode 1	
12.25		7th harmonic of Modes 2 to 5	

6. LOCAL VIBRATION ANALYSIS

Not absolute values of vibration displacements, but relative displacements U_{rel} of the center of the panel formed by web frames are the parameters retained for solving the stated problem in terms of fatigue strength verification for NO96 membrane containment systems. Therefore, the analytic local vibration calculation was performed for cargo tank grillage panels in conditions of supporting contour kinematic excitation at frequencies prevailing in the global vibration spectra alongside with the global ship vibration finite element analysis.

The panel sizes correspond to the distance between the web framing. The calculation was performed by the energy method taking into account the inertia forces of the liquefied gas added masses, the supporting contour submitted to global vibration, and the relative motion of the panel with respect to the supporting contour. The vibro-displacements defined by FEA were considered as supporting contour amplitudes U_{glob}.

For full loaded condition, the calculation was performed by using the following formulae:

$$U_{rel} = \frac{(\Phi_1 + \Phi_2) \cdot U_{glob} \cdot (2\pi\omega)^2}{K_{pr} \cdot \left(1 - \frac{\omega^2}{\lambda^2}\right)}$$

$$K_{pr} = E_{eq} \cdot J \int_0^l \left(\frac{d^2(w(x))}{dx^2}\right)^2 dx$$

$$w(x) = \sin\left(\frac{\pi \cdot x}{l}\right)$$

$$\lambda = \frac{1}{2\pi}\sqrt{\frac{K_{pr}}{M_{pr} + M_{gas\,rel}}}$$

$$\Phi_1 = \frac{M_{pr}}{l}\cdot\int_0^l w(x)dx$$

$$\Phi_2 = \sqrt{M_{gas\,glob}\cdot M_{gas\,rel}}$$

$$M_{pr} = \left(7800\cdot\left(F_r + a\cdot h_s\right) + a\cdot m_{cov}\right)\int_0^l \left(w(x)\right)^2 dx$$

$$M_{gas\,glob} = 470\cdot a\cdot l\cdot H_t$$

$$M_{gas\,rel} = 470\cdot\eta\cdot a\cdot l\int_0^l \left(w(x)\right)^2 dx$$

$$\eta = 1.89\left(\frac{l}{k\cdot a}\right)^4 - 5.49\left(\frac{l}{k\cdot a}\right)^3 + 5.92\left(\frac{l}{k\cdot a}\right)^2 - 2.91\left(\frac{l}{k\cdot a}\right) + 0.90$$

U_{glob} - amplitude of supporting contour displacement (μm)

$w(x)$ - function of stiffener free vibration shape

l - stiffener length (m)

E=2.1·10^{11} steel modulus of elasticity (Pa)

F_r - cross section area of stiffener (m^2)

a - stiffener spacing (m)

h_s - panel plating thickness (m)

m_{cov} - mass of cargo containment system per area (kg/m^2)

H_t - height of liquefied gas column in vibration direction (m)

$M_{gas\,glob}$ - added liquefied gas mass under global vibration (kg)

$M_{gas\,rel}$ - added liquefied gas mass in relative motion (kg)

η_{con} - coefficient of added mass for simply supported continuous plate with side ratio $l/(k\cdot a)$

λ - natural frequency of stiffener (Hz)

ω - frequency of excitation (Hz)

Φ_1 - parameter of reduced inertia force induced by inertia forces of stiffener (kg)

Φ_2 - parameter of reduced inertia force induced by interaction of inertia forces for added liquefied gas masses (kg)

For minimal loading condition, the amplitude of stiffeners' displacement relative to boundaries U_{rel} (μm) was evaluated as following:

$$U_{rel} = \frac{\left(\Phi_1 + \Phi_2^* + \Phi_3\right) \cdot U_{glob} \cdot (2\pi\omega)^2}{K_{pr} \cdot \left(1 - \frac{\omega^2}{\lambda^2}\right)}$$

$$M_{water\ glob} = 1025 \cdot a \cdot l \cdot B_{ballast}$$

$$M_{gas\_water\ rel} = (470 + 1025) \cdot \eta \cdot a \cdot l \int_0^l (u_x)^2\, dx$$

$$\Phi_2^* = \sqrt{M_{gas\ glob} \cdot M_{gas\_water\ rel}}$$

$$\Phi_3 = \sqrt{M_{water\ glob} \cdot M_{gas\_water\ rel}}$$

$B_{ballast}$ was assumed equal to 3.4 m.

Vibration displacements of the center of the panel, which consists of the plating and stiffeners, relative to the supporting contour (web frames), were defined.

Based on the obtained results for each grillage, the spectra containing the greatest vibration displacements at each prevailing frequency were synthesized. The examples of these spectra for two ship loading cases are given in Fig. 6 and 7.

The lowest vibration displacements are observed for the double bottom that could be explained by the high stiffness of this grillage. The maximum levels were observed for the side of tank No.4 that could be explained by great propeller and machinery vibration influence. It should be also noted that the maximum vibration displacements occur under the minimum ship loading case.

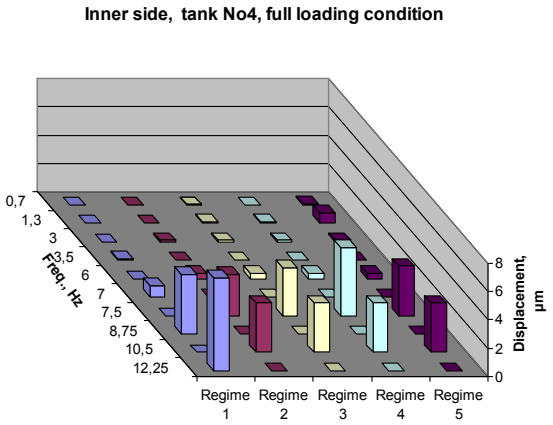

Fig. 6: Example of synthesized spectra for CCS NO96 - Inner side of Tank No.4 - Full loading condition

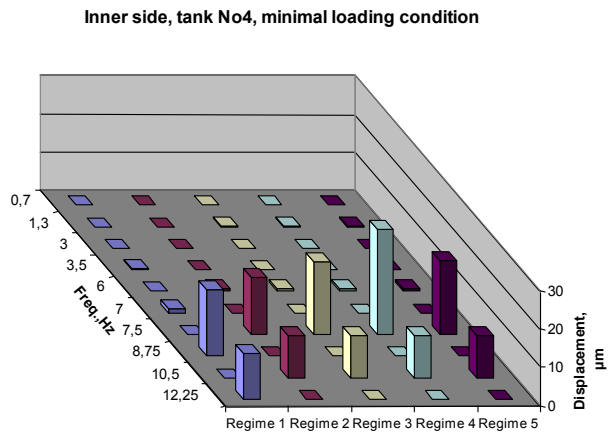

Fig. 7: Example of synthesized spectra for CCS NO96 - Inner side of Tank No.4 - Minimal loading condition

7. GENERATION OF VIBRATION LOADING SPECTRA

Recurrence $N_{i,j}$ depends on the frequency and could be defined by the following formula:

$$N_{i,j} = T_i \cdot \omega_j$$

where T_i = duration of i-th mode

ω_j = frequency of j-th vibro-displacement

The following values were obtained for service life 40 years:

$T_1 = 3.60 \cdot 10^7$ s $\quad T_2 = 4.50 \cdot 10^7$ s $\quad T_3 = 9.00 \cdot 10^6$ s $\quad T_4 = 1.56 \cdot 10^7$ s $\quad T_5 = 3.33 \cdot 10^4$ s

The recurrences of vibration displacements calculated for various frequencies and regimes are given in Table 3.

Table 3.

Cycle numbers of vibro-displacements for various regimes and frequencies under vessel service life 40 years.

Regime No.	1	2	3	4	5
Duration (s)	$3.60 \cdot 10^7$	$4.50 \cdot 10^7$	$9.00 \cdot 10^6$	$1.56 \cdot 10^7$	$3.33\ 10^4$
Frequency (Hz)					
0.7	$2.52 \cdot 10^7$	$3.15 \cdot 10^7$	$6.30 \cdot 10^6$	$1.09 \cdot 10^8$	$2.33 \cdot 10^4$
1.3	$4.68 \cdot 10^7$	$5.85 \cdot 10^7$	$1.17 \cdot 10^7$	$2.03 \cdot 10^7$	$4.33 \cdot 10^4$
3	$1.08 \cdot 10^8$	$1.35 \cdot 10^8$	$2.70 \cdot 10^7$	$4.68 \cdot 10^7$	$1.00 \cdot 10^5$
3.5	$1.26 \cdot 10^8$	$1.58 \cdot 10^8$	$3.15 \cdot 10^7$	$5.45 \cdot 10^7$	$1.17 \cdot 10^5$
6	$2.16 \cdot 10^8$	$2.70 \cdot 10^8$	$5.40 \cdot 10^7$	$9.35 \cdot 10^7$	$2.00 \cdot 10^5$
7	$2.52 \cdot 10^8$	$3.15 \cdot 10^8$	$6.30 \cdot 10^7$	$1.09 \cdot 10^8$	$2.33 \cdot 10^5$
7.5	$2.70 \cdot 10^8$	$3.38 \cdot 10^8$	$6.75 \cdot 10^7$	$1.17 \cdot 10^8$	$2.50 \cdot 10^5$
8.75	$3.15 \cdot 10^8$	$3.93 \cdot 10^8$	$7.88 \cdot 10^7$	$1.36 \cdot 10^8$	$2.92 \cdot 10^5$
10.5	$3.78 \cdot 10^8$	$4.73 \cdot 10^8$	$9.45 \cdot 10^7$	$1.64 \cdot 10^8$	$3.50 \cdot 10^5$
12.25	$4.42 \cdot 10^8$	$5.52 \cdot 10^8$	$1.10 \cdot 10^8$	$1.91 \cdot 10^8$	$4.08 \cdot 10^5$

To evaluate fatigue damage under multi-frequency loading of structures, loading cycles reflecting certain methods for summing amplitudes of different frequencies shall be singled out. To perform this procedure, vibro-displacements of all frequencies were summed with synchronization by time. An example of the obtained realizations (of 20 s duration) is presented in Fig. 8. To define the value and recurrence of total vibro-displacements in the structures under consideration for each regime, the "rain flow method" was used.

The amplitudes histogram $(n_i, U_{rel,i})_{i=1,..,N}$ (n_i number of cycles of amplitude $U_{rel,i}$) obtained through the "rain flow method" was transformed to the single-amplitude one (n, U_{rel}) through the linear damage summation hypothesis [11, 12]: $n = \sum_i \left(n_i \left(\frac{U_{rel,i}}{U_{rel}} \right)^m \right)$

m = coefficient being taken equal to 3.5

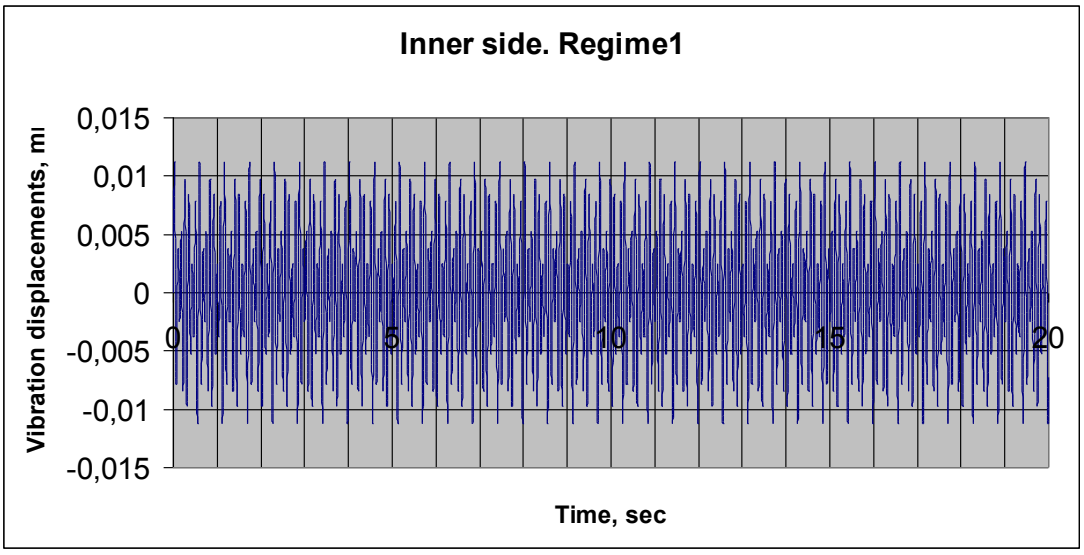

Fig.8: Time history of side structural vibro-displacements for 20 sec, Regime 1

For each considered structure, the operational displacement spectrum was recalculated for the maximum displacement of the corresponding structure. Spectra of equivalent single-amplitude loading were obtained from this recalculation. For further fatigue strength analysis of membrane containment system, the severest ship operation scenario was selected when 50% of the service life the ship operates with full load and 50% of the service life the ship operates under 10% load in the aft tank (tank n°4). The service vibration loading spectrum corresponding to this scenario for the most loaded side grillage structure contains 1.047×10^8 displacement repetition cycles with 0.076 mm range.

8. FATIGUE TESTS OF THE INSULATION BLOCK

A special test bench was developed for experimental estimation of fatigue strength margins for membrane containment systems under ice vibration. This test bench permits the realization of cyclic bending of the full scale ship hull fragment simulating the cargo tank inner side together with the NO96 insulation block (Fig.9).

The insulation block structure was developed by GTT. The insulation block was assembled from standard reinforced components of NO96 insulation. To control the state of the inner structural elements, a system incorporating strain gauges installed on coupler rods for the primary and secondary insulations, as well as cleat displacement sensors installed in both layers were developed. The schematic diagram of the sensor layout is shown in Fig. 10. Totally 18 strain gauges and 40 cleat displacement sensors were installed in the insulation block. The vacuum was created inside the block. The general view of the mock-up prepared for the tests is shown in Fig. 11.

The endurance test program incorporated the following three stages (above linear damage summation theory was applied to accelerate the test, U_{rel} being taken equal to 0.34, 0.41 then 0.67 mm instead of maximal 0.076 mm value): $1x10^6$ loading cycles with deflection 0.34 mm (one life cycle equal to 40 years is simulated), $0.5x10^6$ loading cycles with deflection 0.41 mm (one life cycle equal to 40 years is simulated) and $0.7x10^6$ loading cycles with deflection 0.67 mm (eight life cycles equal to 40 years each are simulated). The total loading number was equivalent to ten ship life cycles.

Prior to the fatigue testing, static tests of the support itself, as well as fully assembled mock-up were conducted. They permitted the establishment of stiffness characteristics of the NO96 membrane containment system required for practical LNGC strength and vibration calculations.

In addition, control dynamic loadings under load application frequencies 1, 3, 5, 7, 9 and 12 Hz and mock-up deflections 0.2 and 0.1 mm were conducted. For each regime the strains in eight secondary insulation couplers were recorded. The analysis of the records showed that the measured parameters do not depend on the loading frequency. No sign of inner resonances was detected within the vibro-displacements frequency range for NO96 membrane containment system in the ice conditions.

After those preliminary tests, endurance test was performed. The measured parameters of the insulation internal state under both static loading and measuring in the real time mode have demonstrated the absence of fatigue damage signs. The coupler strains did not exceed 30-40 μm/m and were at the minimum detectable level of strain gauges. The cleat displacements did

not exceed 0.02 ~ 0.03 mm. After unloading, the readings of the displacement sensor returned to zero. The pressure inside the block remained constant.

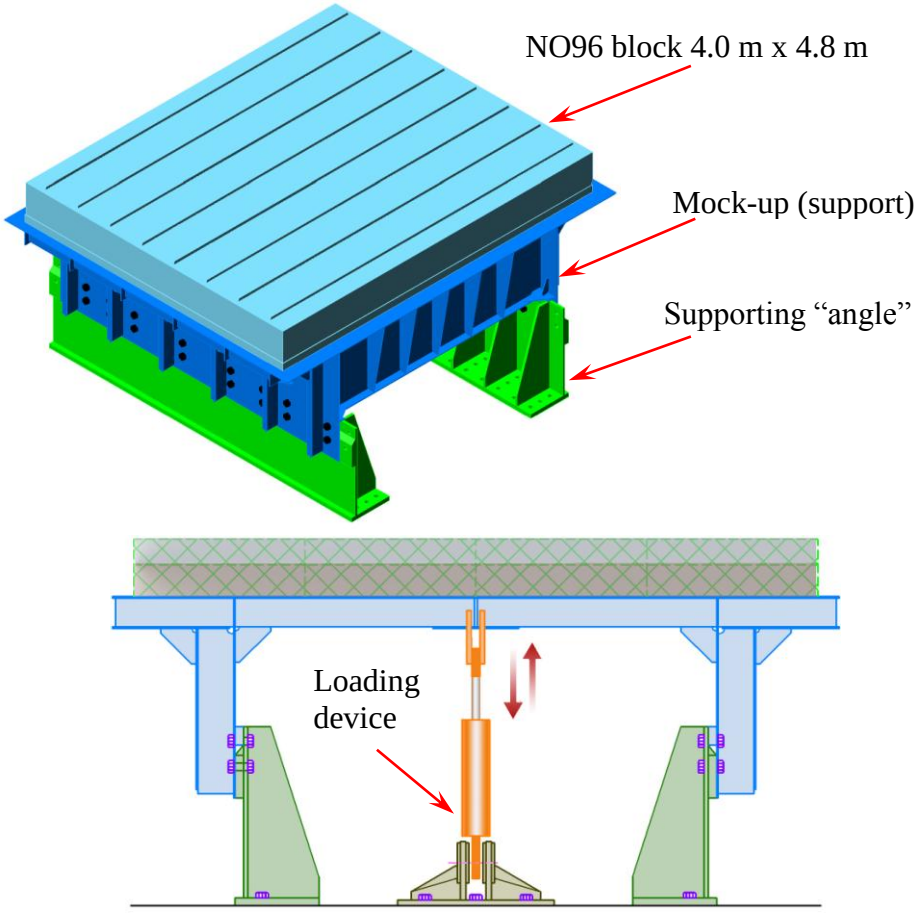

Fig. 9: Side grillage mock-up installed on test bench

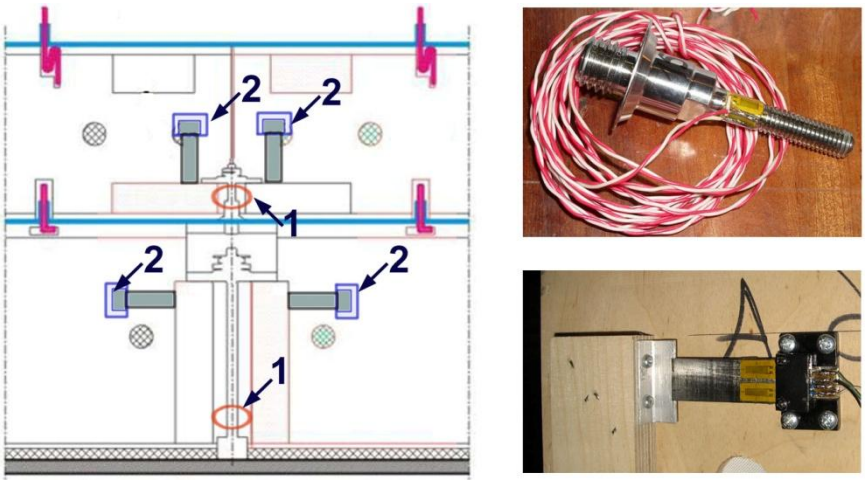

Fig. 10: Schematic diagram of sensor layout inside insulation block

(1 – strain gauge; 2 – cleat displacement sensor)

Primary insulation coupler with installed strain gauge and secondary insulation cleat displacement sensor are shown on the right

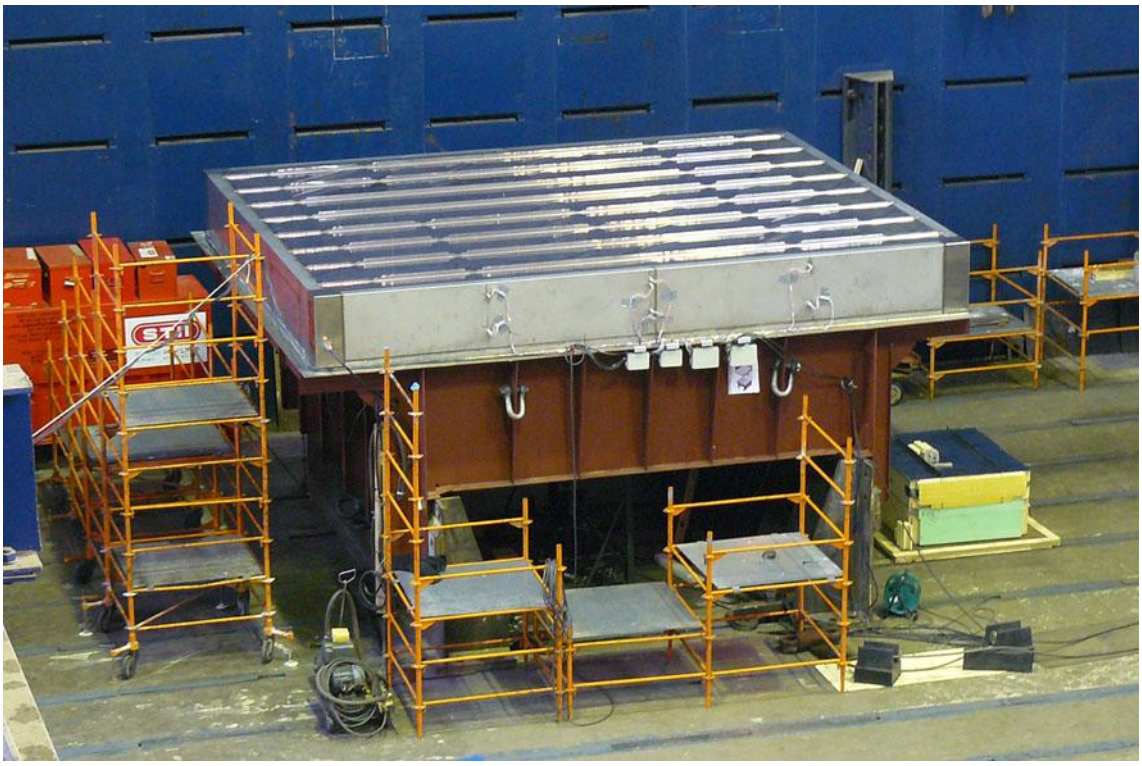

Fig. 11: General view of side grillage mock-up on test bench

9. CONCLUSION

The fatigue strength of NO96 containment system is sufficient for resisting vibration loads occurring at 40-year service life of a large Arctic LNGC in severe ice conditions. The experimentally established fatigue strength margin is more than ten times as great as the service life of a large Arctic LNGC in ice conditions. This demonstrates the suitability of NO96 containment system application for Arctic LNGC.

This project was performed considering that the critical parameter for LNG CCS was the deflection of the inner hull. Complementary tests will be achieved in 2010 to ensure the endurance of the membrane systems under accelerations due to vibration in arctic operations.

REFERENCES

1. Russian Maritime Register of Shipping. Rules for Classing and Building Sea Ships– RMRS, St.Petersburg, 2008.
2. GTT. General Hull Scantling. Maximum Allowable Bending Stress. Extract from N0-DG-33M, 2009.
3. Sazonov K.E. Ship Ice Maneuverability. – Krylov Shipbuilding Research Institute, St.Petersburg, 2006, 252 p.

4. Collection of RMRS Normative Documents, Book 12, 2004.
5. Merculov V., Pasumansky E., Serov A. Ice Loads and Requirements to the Shafts Strength of Icebreakers and Ice-going Vessels. – Proc. of 6th Int. Conf. on Ships and Marine Structures in Cold Regions, ICETECH'2000, St. Petersburg, 2000.
6. Collection of RMRS Normative Documents, Book 14, 2004.
7. Appolonov E.M., Didkovsky A.V., Kopilets N.F., Nesterov A.B. Draft of New Revision of Requirements Contained in Russian Maritime Register of Shipping Rules to Ice Strength of Ships and Icebreakers. – Sudostroenie, No.5, 1997, p.p. 17 – 23.
8. Korotkin A.I.. Added Ship Masses. – Reference Book, L.: Sudostroenie, 1986.
9. Valanto P. Numerical Prediction of Ice Loads and Resistance of Ships Advancing in Level Ice. – Proc. of 6th Int. Conf. on Ships and Marine Structures in Cold Regions, ICETECH'2000, St. Petersburg, 2000.
10. Boudanov D. A., Nikolsky Y A.. Ship Hull Vibrations underway in Ice. – Proc. Of Int. Conf. "On Development and Commercial Utilization of Technologies in Polar Region", St. Petersburg, 1996.
11. ASTM E 468-98. Standard Practice for Presentation of Constant Amplitude Fatigue Test Results for Metallic Materials.
12. Fatigue Assessment of Ship Structures. DNV. Classification Notes No. 30.7. July 2005.